remarkable result is that the entropic barriers arising from the bottlenecks of the system force the chain diffusion to be slower than even reptation. Of course, one might wonder about the crossover from such an entropically activated dynamics regime (with an apparent power law, $D \sim N^{-x}$, $x > 2$) for chains of moderate length to the reptation regime ($D \sim N^{-2}$) for infinitely long chains. Again, questions like what the crossover N and the various amplitudes are and whether this crossover is of any physical interest to a particular experimental situation are very interesting. Simulations for longer chains are in progress in an attempt to answer some of these questions. It is hoped that this simulation study would stimulate tests of the validity of the scaling form presented here for realistic experimental systems.

Acknowledgment. This work was supported by National Science Foundation Grant No. DMR-8420962 and the Materials Research Laboratory at the University of Massachusetts.

References and Notes

(1) Ferry, J. D. *Viscoelastic Properties of Polymers*; Wiley: New York, 1980.
(2) Yau, W. W.; Kirkland, J. J.; Bly, D. E. *Modern Size-Exclusion Liquid Chromatography*; Wiley: New York, 1979.
(3) Bean, C. P. In *Membranes, A Series of Advances*; Eiseman, G., Ed.; Wiley: New York, 1972; Vol. 1.
(4) Dullien, F. A. L. *Porous Media, Fluid Transport and Pore Structure*; Academic Press: New York, 1979.
(5) Tennikov, M. B.; Belenkii, B.; Nesterov, V.; Anaeva, T. *Colloid J. USSR (Engl. Transl.)* **1979**, *41*, 526.
(6) Cannel, D. S.; Rondelez, F. *Macromolecules* **1980**, *13*, 1599.
(7) Guillot, G.; Leger, L.; Rondelez, F. *Macromolecules* **1985**, *8*, 2531.
(8) Bohrer, M. P.; Patterson, G. D.; Carroll, P. J. *Macromolecules* **1984**, *17*, 1170.
(9) Bishop, M. T.; Langley, K. H.; Karasz, F. E. *Phys. Rev. Lett.* **1986**, *57*, 1741.
(10) Graessley, W. W. *Faraday Symp. Chem. Soc.* **1983**, *18*, 1.
(11) Tirrell, M. *Rubber Chem. Technol.* **1984**, *7*, 523.
(12) Kim, H.; Chang, T.; Yohanan, J. M.; Wang, L.; Yu, H. *Macromolecules* **1986**, *19*, 2737.
(13) Phillies, G. D. J. *Macromolecules* **1986**, *19*, 2637; **1987**, *20*, 559.
(14) Renkin, E. M. *J. Gen. Physiol.* **1954**, *38*, 225.
(15) Casassa, E. F. *J. Polym. Sci., Polym. Lett. Ed.* **1967**, *5*, 773. *J. Polym. Sci., Polym. Phys. Ed.* **1972**, *10*, 381; *Macromolecules* **1976**, *9*, 182.
(16) de Gennes, P. G. *Scaling Concepts in Polymer Physics*; Cornell University Press: Ithaca, NY, 1979.
(17) Doi, M.; Edwards, S. F. *The Theory of Polymer Dynamics*; Clarendon Press: Oxford, 1986.
(18) Even, U.; Rademann, K.; Jortner, J.; Manor, N.; Reisfeld, R. *Phys. Rev. Lett.* **1984**, *52*, 2164.
(19) Katz, A. J.; Thompson, A. H. *Phys. Rev. Lett.* **1985**, *54*, 1325.
(20) Dozier, W. D.; Drake, J. M.; Klafter, J. *Phys. Rev. Lett.* **1986**, *56*, 197.
(21) de Gennes, P. G. *J. Chem. Phys.* **1971**, *55*, 572; **1980**, *72*, 4756.
(22) Graessley, W. W. *Adv. Polym. Sci.* **1982**, *47*, 67.
(23) Doi, M. *J. Polym. Sci., Polym. Lett. Ed.* **1981**, *19*, 265.
(24) Muthukumar, M. *Chem. Phys. Lett.* **1982**, *91*, 40.
(25) Deutsch, J. M. *Phys. Rev. Lett.* **1985**, *54*, 56.
(26) Rubinstein, M. *Phys. Rev. Lett.* **1985**, *59*, 1946.
(27) Baumgartner, A. In *Applications of the Monte Carlo Method in Statistical Physics*; Binder, K., Ed.; Springer-Verlag: New York, 1984.
(28) Kolinski, A.; Skolnick, J.; Yaris, R. *J. Chem. Phys.* **1987**, *86*, 1567, 7164, 7174.
(29) Baumgartner, A.; Muthukumar, M. *J. Chem. Phys.* **1987**, *87*, 3082.
(30) Stauffer, D. *Introduction to Percolation Theory*; Taylor and Francis: London, 1985.
(31) Muthukumar, M.; Baumgartner, A. *Macromolecules*, submitted for publication.

Scaling Properties of Branched Polyesters

E. V. Patton, J. A. Wesson,* M. Rubinstein, J. C. Wilson, and L. E. Oppenheimer

Research Laboratories, Eastman Kodak Company, Rochester, New York 14650.
Received June 21, 1988; Revised Manuscript Received September 26, 1988

ABSTRACT: The growth of branched polymer structures up to the gel point has been examined in a polyester system at two different branch agent concentrations. Several independent measurements of the size and molecular weight of these polymers were made using elastic light scattering, quasi-elastic light scattering, intrinsic viscosity [η], and size-exclusion chromatography with low-angle light scattering detection. In all cases, scaling relationships between these various properties were displayed for the whole range of molecular weights examined. The weight-average molecular weight scaled as $(p_c - p)^{-\gamma}$, where p is the extent of reaction and p_c is the extent of reaction at the gel point. The exponent γ was found to be 1.8 ± 0.3. Scaling exponents from the radius–M_w and [η]–M_w relationships were evaluated for unfractionated samples. Using these exponents, another critical exponent of gelation, τ, and the exponent relating size to molecular weight for a branched polymer in a good solvent, ν^B, could be evaluated. These were compared with values for the same exponents obtained through size-exclusion chromatography of the polymers. The critical exponent τ was obtained from this fractionation experiment through the shape of the observed distribution function and from the scaling relation between the molecular weight M_{max}, corresponding to the fraction making the largest contribution to light scattering in this separation, and M_w for each sample. Good agreement was observed between these two separate measures of τ and the one from the unfractionated samples, as well as ν^B from both fractionated and unfractionated samples. The measured values were $\tau = 2.29 \pm 0.03$ and $\nu^B = 0.48 \pm 0.02$. The distribution functions for polymers were described by a single universal distribution function. The critical exponents for gelation were compared to percolation and Flory–Stockmayer predictions and were found to favor the percolation results, but the agreement with percolation for the exponent τ was marginal.

Introduction

Gelation is one of the most interesting and important phase transitions in polymer science and has been the subject of considerable theoretical and experimental study for the past half century. The first theoretical treatment was the mean-field theory developed by Flory[1] and Stockmayer[2] in the early 1940s, which elucidated many key features of the sol–gel transition. Although the mean-field theory did not predict experimental results quantitatively, for a number of years further developments were limited to applying corrections to this classical approach. In the mid-1970s, de Gennes[3] and Stauffer[4] proposed that the

0024-9297/89/2222-1946$01.50/0

percolation model introduced earlier by Broadbent and Hammersley[5] provided a better description of gelation. Both the Flory–Stockmayer and percolation approaches are static theories; they do not take into account the growth rate or the mobility of molecules. Clearly, these kinetic effects are important for certain classes of gelling systems, and separate models have been developed for these circumstances. For instance, the kinetic gelation model[6-8] was recently proposed to deal with growth rate in addition polymerization processes and was tested experimentally with a free-radical-initiated polymerization.[9] The mobility of molecules is taken into account in the clustering of clusters model of gelation.[10,11] Excellent reviews exist for the percolation theory[12,13] and its application to gelation,[14] kinetic models of gelation,[15] and the classical approach,[16] so only the results important to this work are summarized below.

While many experimental studies have been carried out in the last 40 years on gelling systems, only a small fraction of these were designed to test the fundamental predictions of gelation models. The results of a literature search of 300 experimental papers written on gelation between 1963 and 1978 show no clear confirmation of one of the models,[17] but a more recent review of experiments[14] suggests a preference for the percolation model over the Flory–Stockmayer model. In the past few years, several new measurements have been reported[18-20] that strengthen the preference for percolation, but the issue is far from being resolved due to a number of experimental difficulties previously cited[14] and potential differences between behaviors exhibited by the various chemical systems employed.

The current emphasis in experimental studies is on classifying the gelation process. It has been widely accepted in the field of critical phenomena[21] (of which gelation is a particular example) that certain quantities can be used to describe the system, which are independent of the actual materials and of the details of the models employed. These are called universal quantities, and all phase transitions are divided into a small number of universality classes, each characterized by a unique set of universal quantities. Examples of universal quantities are the critical exponents obtained from scaling relationships between one physical property of a system and another near the transition point, e.g., weight-average molecular weight M_w and the distance from the gel point as measured by the extent of reaction. Determining the universality class of a given gelation process has been proposed as the best method for characterizing the sol–gel transition.[13,14] In the present paper, our first priority is to certify the utility of scaling concepts for describing the progress of a gelation reaction. Once the critical exponents have been obtained through scaling relationships, the theoretical predictions are easily evaluated.

We have chosen a polyester made by bulk condensation polymerization as a test system to probe the applicability of the scaling approach, as well as evaluate the predictions of the two available static theories. In this polycondensation, the reaction components are equilibrated through transesterification during the polymerization reaction; this should provide a system that is as close to static conditions as possible. We have specifically chosen a thermally stable, amorphous composition with a glass transition temperature above room temperature to allow for effective quenching of the reaction when sampling the time evolution of the molecular weight distribution. Experiments have been performed to measure the size, molecular weight, and the number of bonds formed (given in terms of the extent of reaction, p) up to the first appearance of gel in the system. In several instances, we were able to evaluate particular scaling or critical exponents through more than one combination of experimental data, allowing us to establish those values with a great deal of confidence for our system. Additional studies have been performed on the polymer microstructure of the same polyesters by NMR, and these are reported in a separate paper.[22]

Scaling and Critical Exponents

The basis for the data analysis described below is the determination of scaling relationships between various experimentally measurable quantities. In the discussion that follows, we define the relations used in the paper and the relevant scaling exponents. It is beyond the scope of this work to review thoroughly all scaling relations for gelation, so only the final results relevant for our measurements are stated throughout the paper. We have used the notation of Stauffer et al.[14] for the scaling exponents.

In polydisperse samples, the scaling of any average quantities with another will in general depend on which average is involved and on the distribution of molecular weights $P(M)$ (the number fraction of molecules of molecular weight M). This distribution is very broad in gelling systems, particularly near the gel point. Different moments of this distribution are given by

$$m_k = \sum_M M^k P(M) \tag{1}$$

where the sum is taken only over finite M. We will use these moments to define the necessary parameters which interrelate the various measurements made on the gelling polymers.

The first moment m_1 is proportional to the density of the sol fraction and therefore is constant (equal to the total density of polymer) below the gel point. For $p > p_c$, m_1 decreases by the gel fraction according to the following two relations:

$$m_1 \sim 1 - G \quad \text{and} \quad G \sim |p - p_c|^\beta \tag{2}$$

where β is the critical exponent relating extent of reaction to the gel fraction G.

The weight-average molecular weight is given by the ratio of the second moment to the first, $M_w = m_2/m_1$. The second moment diverges at the gel point with an exponent γ:

$$m_2 = M_w m_1 \sim |p - p_c|^{-\gamma} \tag{3}$$

Since m_1 is a constant for $p < p_c$, the weight-average molecular weight must diverge as

$$M_w \sim |p - p_c|^{-\gamma} \tag{4}$$

This represents the first directly measurable result in that we can obtain M_w by light scattering and p has been measured by a derivatization technique reported elsewhere.[22] The first and second moments define two critical exponents, β and γ.

Returning to the form of the distribution function, we can find an alternative path to the exponents defined above using the scaling assumption. According to Essam and Gwilym,[23] the distribution of molecular weights for a gelling sample is given by

$$P(M,p) = M^{-\tau} f(M/M_{char}) \tag{5}$$

where f is a cutoff function, τ is a critical exponent, and M_{char} is the characteristic molecular weight for a sample at a particular extent of reaction. This characteristic molecular weight diverges near the gel point, defining another critical exponent σ:

$$M_{char} \sim |p - p_c|^{-1/\sigma} \quad (6)$$

The complete scaling relation can be obtained by combining eq 5 and 6 as

$$P(M,p) = M^{-\tau} f'\{(p_c - p)M^{\sigma}\} \quad (7)$$

This scaling assumption is valid for large molecular weights near the gel point. Of course, different values for the two critical exponents, τ and σ, are obtained from the different theories. The function f' is a cutoff function that defines the way $P(M,p)$ decays to zero at large M ($M \sim M_{char}$) for $p \neq p_c$. The form of f' is difficult to verify experimentally, and we will return to this point in the Results.

We have tested the validity of eq 7 for branched polyesters using size-exclusion chromatography (SEC) with light scattering detection. Leibler and Schosseler[18] first exploited this method in their study of radiation cross-linked polystyrene chains, although the applicability of this form for the distribution function had been examined earlier with a different experimental method by von Schulthess et al.[24]

The scaling assumption (eq 7) relates the exponents τ and σ to the previously defined critical exponents, β and γ. In order to obtain these relationships, eq 7 is substituted into the moment-generating function (eq 1) to yield

$$m_k \sim |p - p_c|^{(\tau-k-1)/\sigma} \quad (8)$$

Evaluating eq 8 for the first and second moments leads to

$$\beta = \frac{(\tau - 2)}{\sigma} \quad (9)$$

$$\gamma = \frac{(3 - \tau)}{\sigma} \quad (10)$$

It is clear from eq 9 and 10 that of the four critical exponents defined so far, only two are independent. We have measured τ and γ, and other exponents can be calculated after we prove the scaling hypothesis (eq 7).

Accurate determination of the gel point p_c is very difficult, but various other quantities can be measured simultaneously and compared with each other. In particular, different measurements of chain size are normally compared to molecular weight to evaluate the growth of branched structures. The experimental techniques used in this study yield four separate measures of the size of the branched polymer structures in dilute solution. Three of the techniques give us quantities equivalent to the hydrodynamic radius, namely, quasi-elastic light scattering (QLS), intrinsic viscosity, and SEC. The results from each of these measures are related to different aspects of the distribution of species in the sample. The simplest to deal with is the SEC result. Since this experiment separates the branched polymer distribution into its various components based on their hydrodynamic volumes, single-chain properties can be calculated once the molecular weight of the eluting species can be established. The QLS and viscosity experiments are both performed on unfractionated samples and therefore give radii corresponding to averages for the sample. The QLS result corresponds to a z-average hydrodynamic radius and the viscosity result to a weight-average quantity.[14] The fourth method for obtaining size, elastic light scattering (ELS), yields a z-average radius of gyration. Since for most dilute solution measurements it is desirable to work in good solvents for the polymer, chain expansion must be accounted for in the correlations between molecular weight and size. As pointed out below, the predicted scaling relationships between these various measurements of size and molecular weight contain both the scaling exponent ν, which is unrelated to gelation exponents, and various combinations of critical scaling exponents for gelation deriving from the fact that different measurements correspond to different averages of the distribution. This exponent ν must be distinguished from the gelation exponent ν defined by Stauffer,[13] which appears in the Discussion. We will use ν_p to designate the gelation exponent.

Table I
Molecular Weight Exponent in Three Dimensions

solvent	linear	randomly branched
good	3/5	1/2
Θ	1/2	7/16

The scaling relationship for the dependence of radius of gyration on molecular weight is given by

$$R_g \sim M^{\nu} \quad (11)$$

where ν is the exponent for a single chain in dilute solution. Flory theory, based on the balance between the excluded-volume and elastic parts of the free energy, predicts that the exponent ν^L for linear polymers[16] and ν^B for randomly branched polymers[25] in good solvents will be

$$\nu^L = \frac{3}{d + 2} \quad \text{and} \quad \nu^B = \frac{5}{2(d + 2)} \quad (12)$$

where d is the dimensionality of space. In a Θ solvent, the exponent for a randomly branched polymer was shown to be $7/4(d + 1)$.[26] With the well-known result of $\nu^L = {}^1/_2$ for linear polymers in three dimensions in Θ solvents, the theoretical predictions for the dependence of size on molecular weight for monodisperse polymers are summarized in Table I. These exponents can be obtained directly from the SEC data, where the distribution has been separated into its component molecular sizes, as described below.

Working from the form of $P(M)$ given in eq 7, Daoud et al.[27] have shown that a diluted polydisperse sample should have the following relation between the z-average radius of gyration $\langle R_g \rangle_z$ and the weight-average molecular weight:

$$\langle R_g^2 \rangle_z \sim M_w^{2\nu_e} \quad (13)$$

where ν_e is the effective ν given by

$$\nu_e = \nu^B/(3 - \tau) \quad (14)$$

This relationship should also apply to the hydrodynamic radius R_h obtained from QLS, since it is also a z-average quantity and is proportional to R_g.[28] The exponent ν_e contains information on both the solvent quality through the exponent ν^B, as illustrated in Table I, and the distribution of molecular weights through the critical exponent τ. To separate the two factors from each other, the results from intrinsic viscosity must be used. The intrinsic viscosity, $[\eta]$, of a monodisperse polymer should scale as the specific volume of the solvated polymer as

$$[\eta] \sim R^d/M \quad (15)$$

or in terms of molecular weight as

$$[\eta] \sim M^{3\nu-1} \quad (16)$$

Again, Daoud et al.[27] have formulated the relationship between the average quantities observable in experiments on a diluted system as

$$[\eta] \sim M_w^{(3\nu^B-\tau+1)/(3-\tau)} \quad (17)$$

where a different combination of ν^B and τ appears. The combination of eq 13, 14, and 17 can be used to obtain the values of the individual exponents.

Table II
Theoretical Predictions of Critical Exponents

	β	γ	σ	τ
Flory–Stockmayer	1	1	1/2	5/2
percolation (d = 3)	0.4	1.8	0.45	2.2

All static critical exponents of the gelation transition can be determined from a set of three independent ones using the scaling relations. In the experiments reported in this study, we can measure only two independent critical exponents, γ and τ, and on the basis of the scaling hypothesis, we can calculate several others that are related to these two exponents. The third independent critical exponent can be obtained if we assume hyperscaling (see Discussion), but we are unable to verify this assumption experimentally. We can, however, test the internal consistency of this data analysis protocol by comparing the values for a critical exponent obtained through different measurements. The two theoretical predictions for all the critical exponents defined above are summarized in Table II.

Experimental Section

Synthesis. Numerous samples were prepared at each of two different levels of pentaerythritol as a branch agent in a melt condensation reaction. Each synthesis was carried out in a two-step process. In the first step, stoichiometric quantities of dimethyl terephthalate, dimethyl glutarate (added to reduce crystallinity), and pentaerythritol were mixed with a 40% excess of neopentyl glycol and a catalyst. This mixture was heated to 220 °C for 1–2 h under nitrogen at ambient pressure to exchange all the methyl esters with either the linear or branching alcohol monomer. In the second step, the mixture at elevated temperature was placed under vacuum to remove excess neopentyl glycol from subsequent ester-exchange reactions, leading to buildup of the polymer molecular weight, for approximately another hour. These steps were designed to yield a polymer with the following molar composition: terephthalate (0.95), glutarate (0.05), neopentyl glycol ($1 - 2X$), and pentaerythritol (X), where X was either 0.025 or 0.05. A typical synthesis is described in detail below. Also, a series of linear polyesters with neopentyl glycol and the same 95/5 molar ratio of terephthalate to glutarate moieties but different molecular weights were prepared by the same general procedure to calibrate the SEC experiment.

A mixture of 332.1 g (1.71 mol) of dimethyl terephthalate, 14.4 g (0.09 mol) of dimethyl glutarate, 253.2 g (2.43 mol) of neopentyl glycol, and 6.13 g (0.045 mol) of pentaerythritol was weighed into a 1-L three-necked flask equipped with a nitrogen inlet tube and a metal blade stirrer. The third neck was used for sampling the reaction mixture. The mixture was heated to 220 °C until molten. Tetraisopropyl orthotitanate (18 drops) was added as a catalyst, and the mixture was agitated at 220 °C for 2 h under ambient pressure of nitrogen and for an additional hour at 240 °C. The pressure was then reduced to 0.1 mmHg to remove the excess neopentyl glycol resulting from further ester-exchange reactions. As the molecular weight built up under vacuum, samples (approximately 5 g each) were removed from the mixture by breaking the vacuum and inserting a metal blade spatula. Samples were removed at 15 min intervals from 0 to 75 min, placed in a sealed vial, and allowed to cool to room temperature under ambient conditions, quenching the reaction.

Elastic Light Scattering. Scattering measurements were carried out in distilled tetrahydrofuran by using a C. N. Wood multiangle light scattering photometer. The polymer solutions were filtered through Millipore Corp. 0.5-μm Millex-SR filter units prior to measurement. Scattering intensities at 436 and 546 nm were typically measured at eight angles from 40° to 130° and at four concentrations. Molecular weights, radii of gyration, and second virial coefficients were determined from Zimm plots of the scattering data by the normal extrapolation techniques. A Zimm plot representative of a typical data set is shown in Figure 1. They tended to be rectilinear with minimal curvature in the angular dependence, consistent with the predicted form of the scattering envelope for random f-functional polycondensation.[29]

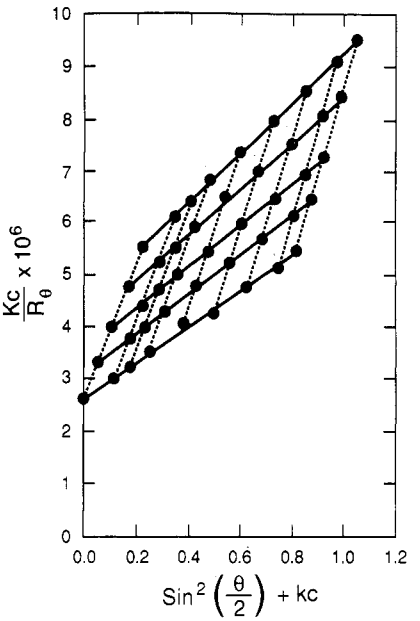

Figure 1. Zimm plot of the light scattering at 436 nm for sample 91F. Scattering intensities were determined at four concentrations and eight angles; the figure includes points found by extrapolation to $c = 0$ and $\theta = 0$.

If any curvature appeared, the limiting slope at small angles was used. In some cases, an LDC Milton Roy (Chromatix) KMX-6 light scattering photometer (LALLS), which uses a He–Ne laser (632.8 nm) as a light source and measures the scattered intensity at 6.5°, was used for molecular weight and second virial coefficient determinations. The measured scattered intensity was assumed to be the same as a zero-angle value for the LALLS instrument. The two different scattering instruments gave equivalent results on identical samples, but the LALLS instrument, which requires much less material, was used for those samples available in limited quantities. The refractive index increment was measured for several branch agent concentrations and extents of reaction, and it was found to be independent of these variables.

Quasi-Elastic Light Scattering. Polymer solutions were prepared by dissolving weighed amounts of polymer in tetrahydrofuran (EM Industries, chromatography grade) to yield a known volume. Additional concentrations were prepared by successive dilution. All solutions were filtered through Millipore Corp. Millex-SR 0.5-μm filter units prior to measurement. QLS (photon correlation spectroscopy) measurements were carried out with a Brookhaven Instruments Corp. BI 240 goniometer and BI 2030 correlator (128 channel). An Innova 90-4 argon ion laser (Coherent Radiation Corp.) at 514.5 nm was used as a light source. The sample cell was thermostated at 25 °C, and measurements were performed over the angular range from 30° to 90° in 10° increments. Typically, four concentrations between 0.05 and 0.001 g/mL were examined for each polymer. Cumulant analysis was used to calculate the decay constant, Γ, of the correlation function for each measurement. The apparent diffusion coefficient at each concentration was then obtained by linear least-squares analysis of the dependence of Γ on κ^2, where κ is given by

$$\kappa = \frac{4\pi n \sin(\theta/2)}{\lambda_0} \tag{18}$$

where n is the solvent refractive index and λ_0 is the wavelength of the incident light in vacuum. The linear dependence was valid to at least 60° in every case. Finally, the apparent diffusion coefficients obtained from the slopes at each concentration were plotted against concentration, and the infinite dilution value of the diffusion coefficient was obtained by the usual extrapolation. The Stokes–Einstein relation was used to convert the z-average diffusion coefficient to a hydrodynamic radius by

$$R_h = kT/6\pi\eta D_0 \tag{19}$$

where η is the viscosity of tetrahydrofuran.

Viscometry. Viscosities were measured for polymer solutions in distilled tetrahydrofuran at four concentrations using an

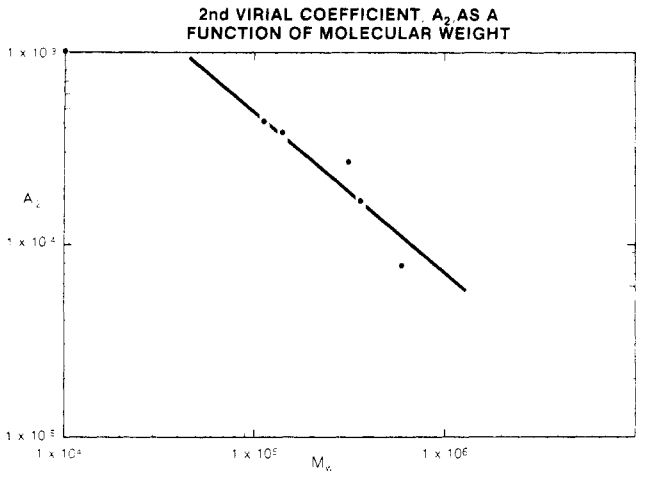

Figure 2. Variation of log A_2, the second virial coefficient, with log M_w for highly branched samples. The relationship described empirically by the straight line drawn in the figure was used to calculate the value of A_2 for each chromatographic increment.

Ubellohde capillary viscometer. Intrinsic viscosities were determined by extrapolation of inherent and reduced viscosities to their common intercept at zero concentration.

Size-Exclusion Chromatography. Polymers were fractionated by SEC in distilled tetrahydrofuran on column sets consisting of 10^6-, 10^5-, 10^4-, and 10^3-Å pore size μ-Styragel columns (Waters Associates, division of Millipore Corp.). The eluting polymer concentration was measured with a Waters Associates R-401 differential refractive index detector, and the light scattering from each increment was measured with a Chromatix low-angle laser light scattering (LALLS) photometer connected directly to the outlet of the columns. Each separation was corrected for the effects of axial dispersion, assuming the band broadening was Gaussian and constant across the molecular weight distribution.[30] The injection concentrations were kept low enough to eliminate elution volume variation due to polymer chain overlap.[31] Flow rates were kept at 1 mL/min, which, combined with the low concentrations, minimized the possibility of shear degradation in the chromatograph.

By combining the information from the concentration and light scattering detectors, the absolute molecular weights of the eluting polymers can be evaluated. Because of the small scattering angle monitored by the LALLS photometer, it was assumed that no angular extrapolation was required. The molecular weight of each fraction was calculated from the following equation:

$$\frac{Kc_i}{R_\theta} = \frac{1}{M_{wi}} + 2A_{2i}c_i \tag{20}$$

where c_i is the concentration in that fraction; R_θ is the Rayleigh ratio; K contains the contributions from geometric factors, wavelength, solvent refractive index, and the refractive index increment; M_{wi} is the weight average molecular weight of that increment; and A_{2i} is the second virial coefficient for that increment. Since A_{2i} is very difficult to measure directly, we have approximated it by using the A_2 versus M_w relationship obtained from broad distribution samples, as shown in Figure 2. The functional form used in eq 20 is represented by the solid line through the data. (We also note that Adam et al.[20] have used this dependence to calculate scaling exponents, but we feel our data are too limited to use this analysis.) The corrections were small for the high molecular weight fractions and use of this approximation for A_{2i} should not cause significant errors;[32] following this procedure we obtain the same value for M_w by SEC as we do by direct measurement on the unfractionated sample with light scattering.

Extent of Reaction Determination. Since the polymerization method should yield a polymer which has all hydroxyl end groups at any point in the reaction, the extent of reaction in each sample was measured by derivatizing the hydroxyl end groups with a trifluoroacetylating agent, followed by ^{19}F NMR of that sample to quantitate the end groups. The detailed procedure for this measurement is given in a separate paper[22] and will not be discussed further here.

Table III
Experimental Measures of Unfractionated Branched Polymers

sample	p	$10^{-3}M_w$	$[\eta]$, dL/g	R_g, nm	R_h, nm
		0.025 MFBA Samples			
183B	0.68	3.8			
183C	0.75	7.0			
183D	0.83	16	0.143		
183E	0.88	280	0.323	51	20
125D		9.5	0.111		
125E		20	0.155	7.5	4.3
125F		110	0.235	23	
125	0.88	114	0.24	27	14
173		34		13	
182-5		140	0.288	29	15
171	0.93	370	0.331	56	34
155	0.90	780	0.478	83	51
		0.05 MFBA Samples			
191B	0.52	2.8			
191C	0.70	5.5			
191D	0.73	9.9			2.9
191E	0.74	12			3.2
191F	0.80	32	0.148		5.9
91A	0.61	5.2			
91B	0.67	6.4			
91C	0.70	12			2.4
91D	0.73	22	0.122		4.6
91E	0.77	57	0.158	16	8.2
91F	0.81	380	0.235	49	29
33C	0.77	22	0.132	16	
33D		660	0.290		

Results

Scaling of Diluted, Unfractionated, Branched Polyesters. Five separate measures of the branched polymer growth can be made on an unfractionated sample with the techniques described above, namely, the extent of reaction, p; the weight-average molecular weight, M_w; the intrinsic viscosity, $[\eta]$; the z-average radius of gyration, R_g; and the z-average hydrodynamic radius R_h. Equations 4, 13, 14, and 17 describe the interrelationships between these variables, as well as definitions for the two independent critical exponents. Table III summarizes the experimental measurements for a number of samples at both 0.025 and 0.05 mole fraction branch agent (MFBA), representing several independent polymer syntheses. There are absences in the data presented, which resulted from having insufficient sample to do all the necessary measurements; however, there are samples for which all measurements have been made. These samples not only provide continuity between the different types of fits to the data but also demonstrate the repeatability of these syntheses, because of the smooth meshing of these points in each fitting format. The comparative analyses are discussed in detail below.

The correlation of M_w with p, as described in eq 4, gives the critical exponent γ directly, but this fit also requires definition of p_c, the extent of reaction at the gel point. Unlike the exponent γ, the critical extent of reaction depends on the composition, so the 0.025 and 0.05 MFBA data must be fit separately. As illustrated in Figure 3 in a plot of log M_w versus p, the 91 series and the other 0.05 MFBA samples describe two distinctly different growth curves, presumably due to some undetected compositional difference. Consequently, these two different sets of 0.05 MFBA data had to be fit separately. Each data set was fit by nonlinear regression with a three-parameter function of the form

$$\ln (M_w) = -\gamma \ln (p_c - p) + \ln B \tag{21}$$

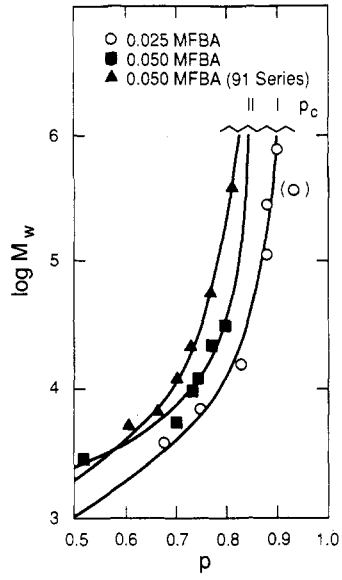

Figure 3. Variation of log M_w with p, the extent of reaction, for samples containing 0.025 MFBA and two different sets of samples containing 0.05 MFBA. Marks are included indicating the fitted value of p_c, the critical extent of reaction or gel point, for each data set.

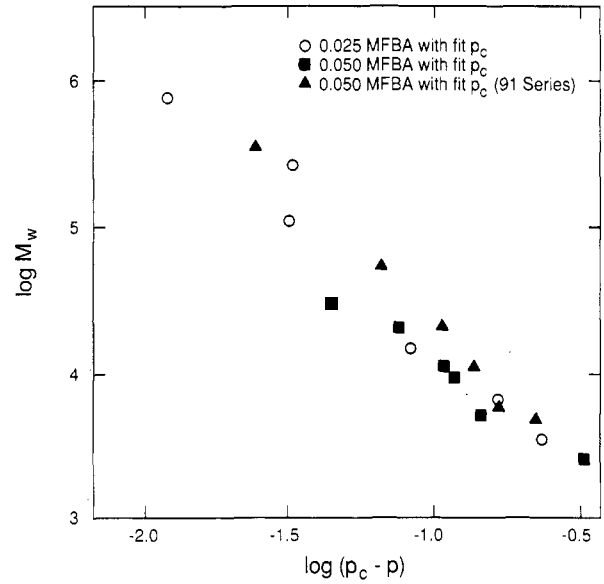

Figure 4. Data points from Figure 3 replotted as log M_w versus log ($p_c - p$). This plot emphasizes the power law relationship between the weight-average molecular weight and the approach to the gel point measured by ($p_c - p$). Although the plots are not colinear, they have similar slopes.

Table IV
Fit Parameters for the Correlation between M_w and p

data set	ln B	γ	p_c
0.025 MFBA	5.2 ± 2.8	2.0 ± 1.3	0.912 ± 0.017
0.050 MFBA, w/o 91 series	6.4 ± 1.7	1.3 ± 1.2	0.844 ± 0.074
0.050 MFBA, 91 series	5.4 ± 1.9	2.0 ± 1.2	0.834 ± 0.034

where B is a constant representing the unspecified prefactor in eq 4. The fit lines for each data set are also shown in Figure 3, and the fit parameters are tabulated in Table IV with estimations of the individual confidence intervals at 95%. The value of p_c in each case is reasonably well defined, but the other two parameters are more sensitive to the limited data ranges.

In the fit of the 0.025 MFBA data set, the point at p = 0.93 (bracketed by parentheses in Figure 3) could not be included, since the function in eq 21 is undefined for values of $p > p_c$ and any sensible fit gives $p_c < 0.93$. This apparently anomalous data point is most likely due to experimental error in the measurement of p, which is about 5%, but it could also represent a similar chemical variation to that seen in the 91 series in the 0.05 MFBA samples. In either case, the measurement of p does not affect the other techniques employed, so this point is included in subsequent analyses.

Our main interest is in obtaining an estimate for γ and some idea of the precision of that estimate. Using the fit values for p_c, these data can be replotted as log M_w versus log ($p_c - p$) to emphasize the power law relationship between these variables, as shown in Figure 4. While the three separate data sets do not appear to form a single line in this plot, they do have similar slopes, i.e., a similar exponent γ. In fact, the values of γ obtained from the nonlinear regression analysis are all within experimental error of one another as seen in Table IV, although the uncertainties are so large that this comparison does not seem very significant. These large uncertainties reflect not only the expected experimental variation but also the limited number of data points in each individual set, so we would like to find the best average value for the data sets.

In order to properly weight the different ranges spanned in each of the data sets, we decided first to normalize the

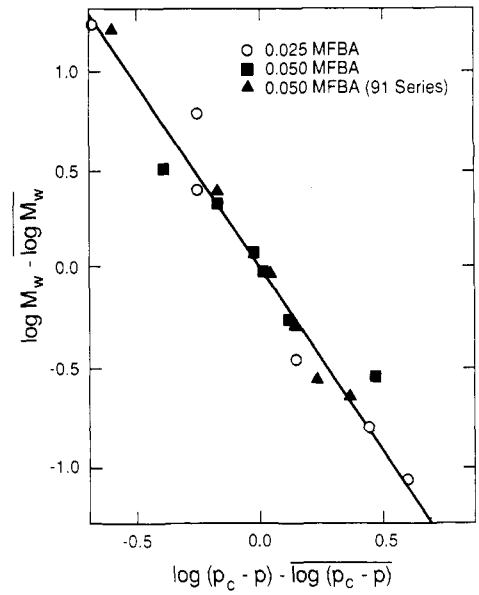

Figure 5. Data from Figure 4 normalized by shifting the midpoint of each data set to the origin. The best value for the slope, γ, describing all the data can then be obtained by linear regression. A value of γ = 1.8 ± 0.3 was found by this procedure.

data sets and then find the best-fit line through the combined data. To avoid artificially changing the weighting of one data set relative to another, we shifted the data sets so that their midpoints corresponded, rather than either of the end points. This procedure involves determining the average log M_w and the average log ($p_c - p$) for each data set and the subtracting these average values from the log M_w and log ($p_c - p$) for each data point in the set. The result leaves the data points equally distributed about the origin, as illustrated in Figure 5, but we have eliminated differences between data sets due to prefactors or p_c values. The best-fit slope to the combination of all three data sets can then be calculated by a simple linear regression analysis, and 95% confidence intervals about this slope were evaluated by using Student's t distribution after reducing the number of degrees of freedom by six (three for

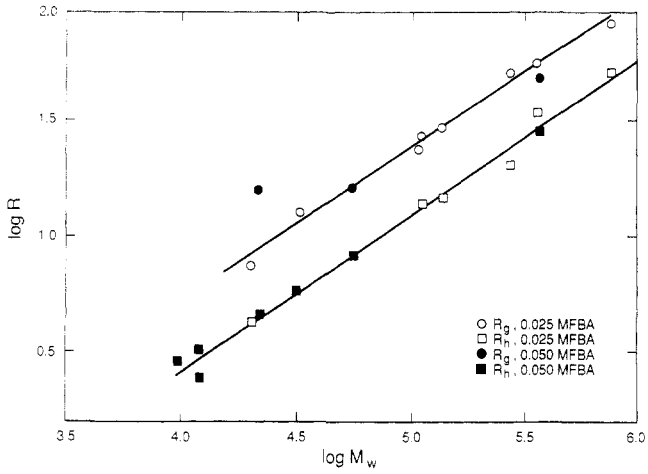

Figure 6. Values of log R_g from elastic light scattering and log R_h from quasi-elastic light scattering plotted for samples containing 0.025 and 0.05 MFBA versus log M_w. The polymers have the same average radii, independent of MFBA. The separate plots of R_g and R_h have the same slopes, indicating that they both scale with log M_w in the same way.

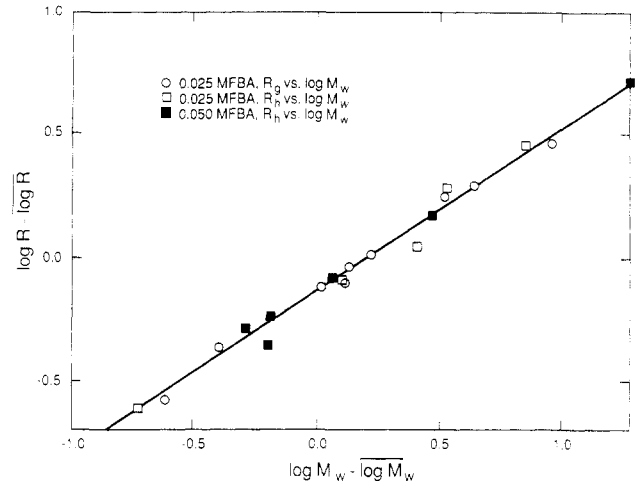

Figure 7. Data from Figure 6 normalized by shifting the midpoint of each data set to the origin. The R_g data at 0.05 MFBA were not included. The slope of this line gave a value for the scaling exponent $\nu_e = 0.66 \pm 0.04$.

using the fit p_c value and three for the normalization procedure). The result of

$$\gamma = 1.8 \pm 0.3 \tag{22}$$

is in excellent agreement with the percolation prediction (Table II). This result was not substantially affected by excluding those points where $p - p_c$ is less than the uncertainty in the value of p. If the existence of this power law defines the bounds of the critical region, then all of our observations are within the critical region, and the critical region is very broad for this system. This feature is born out in other data analyses as well. It will be also shown in subsequent analyses that the value of p_c for a particular reaction condition is one of the few unique parameters observed in these systems; i.e., all other correlations between sizes and molecular weights show no distinctions between the two subsets of the 0.05 MFBA samples and generally no distinctions between any of the branched polymers regardless of MFBA.

Comparisons of radius, viscosity, and molecular weight determinations in unfractionated samples are much better suited to characterizing the gelation transition. While the typical experimental errors in these measurements are also about 5–10%, these variables appear directly in the scaling relationships, so the relative errors do not change when using the scaling approach. On the other hand, scaling relationships involving p are always expressed in terms of the distance from the gel point, $|p_c - p|$, so the experimental errors rapidly exceed the value of the relevant scaling parameter as the gel point is approached. In addition, the radius and molecular weight of a gelling system can change by orders of magnitude near the gel point, making them much better parameters for characterizing gelation. Consequently, all subsequent scaling analyses will use relationships between these direct measures of the system.

The first such relation is defined by eq 13, where the z-average radius of gyration is related to the weight-average molecular weight for an unfractionated sample. The scaling exponent ν_e is given by the combination of ν^B and τ in eq 14. The data for R_g and R_h are plotted versus M_w in Figure 6 in a log–log format for both MFBA levels. Two significant observations are immediately obvious. First, the slopes of the curves of log R_g and log R_h as a function of log M_w are apparently identical, as expected, so either measure of radius will serve for the scaling exponent analysis. The second point is that the radius at a particular molecular weight is apparently independent of the MFBA level. Daoud and Joanny[26] have predicted that R_g depends very weakly on the branch agent concentration. In particular, they state that $R_g \sim (1/\Lambda)^{0.1}$ for a mixture of bifunctional and trifunctional monomers in three dimensions, where Λ^{-1} is proportional to the average number of bifunctional monomers between branch sites. According to their prediction, a factor of 2 change in branch agent concentration would only effect R_g by about 7%, which is probably undetectable in our measurement. It is also clear from these data that R_h is related to R_g by a scalar constant for these polymers in tetrahydrofuran.[34]

Since the critical exponent for the radius–molecular weight relationship is apparently identical for either R_g or R_h measurements (the slopes are 0.66 ± 0.06 for R_g data and 0.67 ± 0.04 for R_h data), we have chosen to calculate our best estimate of ν_e in a manner consistent with the previous analysis. The average log R and log M_w values were calculated separately for the R_g data set at 0.025 MFBA, the R_h data set at 0.025 MFBA, and the R_h data set at 0.05 MFBA, with the shifted result as shown in Figure 7. The R_g data at 0.05 MFBA were not used in this process, because there were too few data points to clearly establish the relationship between R_g and M_w in this case. We found the value of the scaling exponent to be

$$\nu_e = 0.66 \pm 0.04 \tag{23}$$

This value of ν_e is within the confidence interval of, although slightly larger than, the value $\nu_e = 0.58 \pm 0.06$ reported by Leibler and Schosseler[39] in their studies of branched polymers formed by radiation cross-linking of polystyrene solutions. It also agrees with the value of 0.62 ± 0.03 found by Adam et al.[20] in the polyurethane system, although not with the value of 0.5 found by Kajiwara et al.[33] in a different polyurethane system. Finally, Burchard et al.[36] show values in the range 0.42–0.71 in an epoxy system. All the reported values of ν_e are substantially closer to the percolation prediction for $\nu_e = 0.5/(3 - 2.20) = 0.625$ than to the Flory–Stockmayer value of 1 (from eq 14).

The last relation obtainable from our data on unfractionated samples is the combination of critical and scaling exponents given in eq 17, which defines the scaling law for the dependence of $[\eta]$ on M_w. The relevant data from Table III are plotted in Figure 8 as log $[\eta]$ versus log M_w. Also included in Figure 8 are viscosity results for the linear analogues, which are summarized in Table V. Here, the

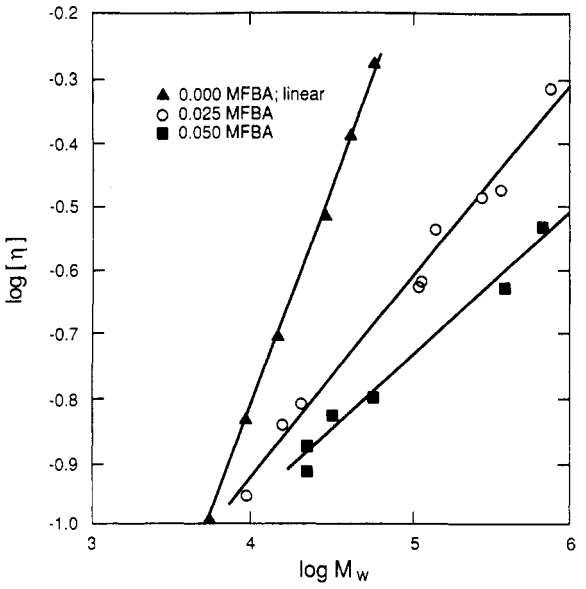

Figure 8. log $[\eta]$ versus log M_w for linear samples and branched samples containing 0.025 MFBA and 0.05 MFBA. The dependence of intrinsic viscosity on M_w varies with MFBA, presumably because $[\eta]$ depends more strongly on the lower moments of the distribution which are more sensitive to the amount of branch agent present.

Table V
Intrinsic Viscosity and Molecular Weights for Linear Polyesters

sample	M_w[a]	M_n[a]	$[\eta]$[b]
21	5410	3300	0.101
23	9270	6400	0.146
25	14100	9040	0.195
27	29600	20100	0.303
29	42500	27200	0.405
67	58600	36300	0.526

[a] Molecular weights were determined by SEC with LALLS detection. M_n values were confirmed by ^{19}F NMR end-group analysis.[22] [b] Intrinsic viscosities were determined at 25 °C in tetrahydrofuran, and they are given in dL/g.

two different MFBA levels appear to define unique viscosity–molecular weight relationships, distinguishable from each other and from the linear polymers. At first sight, this result seems to contradict the behavior seen in the R_h–M_w relationship above, where the two MFBA series were apparently identical. However, $[\eta]$ corresponds to a molecular weight average between M_n and M_w. Consequently, it depends much more strongly on the low molecular weight end of the distribution, which must be composed of a mixture of linear and branched structures with only a few branches (i.e., molecular weights less than 20000). Therefore, the intrinsic viscosity measurement is expected to be more sensitive to the differences resulting from the MFBA level.[32,36]

The calculated scaling exponents for the individual curves are 0.30 ± 0.03 for the 0.025 MFBA series and 0.23 ± 0.04 for the 0.05 MFBA series. However, neither of the theories provides any justification for this exponent depending on the branch agent concentration in the sample, so we have chosen to calculate an average value for this exponent by the same general procedure as above. The results of the data shifting are shown in Figure 9 along with the fit line. The calculated scaling relationship from eq 17 is then

$$\frac{3\nu^B - \tau + 1}{3 - \tau} = 0.28 \pm 0.03 \qquad (24)$$

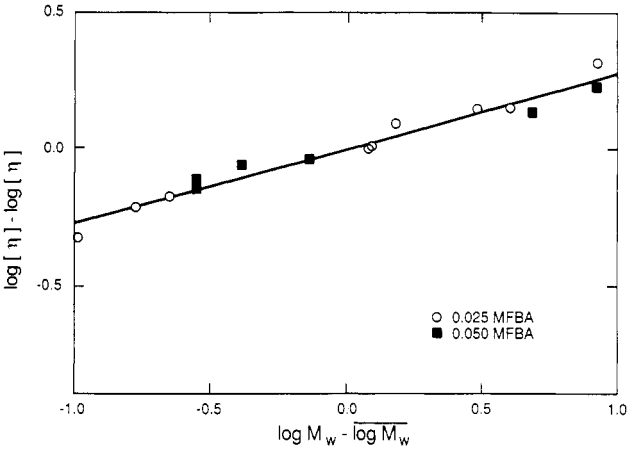

Figure 9. Data from the branched samples in Figure 8 normalized by shifting the midpoints of each data set to the origin. The slope of the line was found to be 0.28 ± 0.03.

The 0.025 MFBA data are, in effect, weighted more heavily, due to the broader range spanned by these data. The confidence interval is surprisingly small, which suggests that the two lines are statistically less different than they appear to be in Figure 8.

The experimental results quoted in eq 23 and 24 provide us with sufficient information to evaluate the scaling exponent ν^B and the critical exponent τ separately. Designating the scaling exponent for the viscosity–molecular weight relationship in eq 24 as υ, we can develop relationships for ν^B and τ in terms of experimentally measured quantities:

$$\nu^B = \frac{2}{3 + ((1 - \upsilon)/\nu_e)} = 0.49 \pm 0.01 \qquad (25)$$

and

$$\tau = 2 + \frac{1}{1 + (2/(3\nu_e - 1 - \upsilon))} = 2.26 \pm 0.04 \qquad (26)$$

where the error limits again represent the 95% confidence intervals following standard propagation of error techniques. The relative errors associated with ν^B and τ are smaller than those for the experimentally obtained quantities due to the number of constants appearing in eq 25 and 26. The value of ν^B is in very good agreement with the Isaacson and Lubensky prediction[25] of the Flory exponent for a randomly branched polymer in a good solvent, $\nu^B = 0.5$ (see eq 12 and Table I). The value of τ is definitely smaller than the Flory–Stockmayer prediction of 2.5, and it is apparently larger than the percolation prediction of 2.20. However, given the error limits normally associated with the numerical evaluations of τ, we cannot be certain whether it agrees or disagrees with this theoretical result.

Scaling of Diluted, Fractionated, Branched Polyesters. The exponents ν^B and τ are directly accessible by fractionating the branched polyester samples; the former through the relation in eq 11 and the latter by two methods outlined below. SEC is obviously the method of choice for this type of study, as elegantly demonstrated by Leibler and Schosseler.[18] However, this technique is not without its caveats. In particular, as the polyesters approached the gel point, they became increasingly sensitive to shear degradation, due to the presence of extremely high molecular weight chains in these samples. We were able to confirm that our results were free of shear degradation problems by establishing that our separations were independent of flow rate. A second problem, noted by Leibler

and Schosseler,[18] is that the distribution is separated into fractions containing chains of equal hydrodynamic volume, which are, furthermore, convoluted with adjacent bands eluting from the column set. Although a correction has been applied for the effects of mixing due to diffusional processes (band broadening) during the separation, a chromatographic fraction may still contain a mixture of molecular weights with different branch contents but the same hydrodynamic volume. With concentration and light scattering detectors, the weight-average molecular weight of the eluting fraction is determined with no regard for the possible breadth of the distribution in the fraction. We are forced to use the same assumption invoked earlier;[18] namely, the statistical nature of the distribution of branch sites makes it unlikely that this mixture is very broad. Certainly, this approximation is best for the high molecular weight end of the distribution and higher extents of reaction: the region we are most interested in. Within these constraints, we then have information on the quantity and molecular weight of polymer for a number of fractions corresponding to equal increments of elution volume, the size of a volume increment having been chosen arbitrarily to yield 20–50 increments across the distribution. The discussion that follows describes how we extracted first ν^B then τ, from these data.

To obtain ν^B, we must know at least the relative sizes of these polymers. Typically, the chromatographic system is calibrated with a set of standards, narrow distribution polymers of known molecular weights, to establish the relationship between molecular weight and elution volume. In this study, the molecular weights are obtained directly through the use of the light scattering detector, but the standards are still necessary to provide information about the relationship of hydrodynamic size to elution volume. According to the Flory–Fox relationship, the hydrodynamic volume of a polymer can be described as[40]

$$R^3 \sim [\eta]M \tag{27}$$

Equation 27 provides the basis for universal calibration of the chromatographic system in that a plot of log ($[\eta]M$) versus elution volume for a given column set is independent of chemical composition or branching for most polymers.[41]

In a typical calibration process, the intrinsic viscosity is replaced by the Mark–Houwink relationship, $[\eta] = KM^a$, where K and a are constants measured independently for the standards in the same solvent. By substituting the Mark–Houwink relation into eq 27, the scaling relation between radius and molecular weight for fractionated samples is obtained directly as

$$R^3 \sim M^{(1+a)} \sim M^{3\nu} \tag{28}$$

Also, knowing the Mark–Houwink relations for two different polymers, the molecular weight of one polymer eluting at a particular volume can be calculated in terms of the other polymer, if its elution volume–molecular weight relation is known, by using

$$\log M_2 = \left(\frac{1}{1+a_2}\right)\log\left(\frac{K_1}{K_2}\right) + \left(\frac{1+a_1}{1+a_2}\right)\log M_1 \tag{29}$$

where the subscripts 1 and 2 designate the first and second polymer, respectively.

In this study, two sets of "standards" were used to establish the calibration curve. First, a series of six linear polyesters with the same diacid content were polymerized with neopentyl glycol to be used as standards. The weight- and number-average molecular weights, as well as the intrinsic viscosities in tetrahydrofuran, are recorded in Table V, and the Mark–Houwink relation is illustrated in Figure 8 by a plot of log $[\eta]$ versus log M_w. The Mark–Houwink parameters were found to be $K = (2.9 \pm 0.2) \times 10^{-4}$ dL/g and $a = 0.68 \pm 0.04$. Values of log M versus V_e, elution volume (in milliliters), taken from SEC fractions of these polymers, were used to construct the linear calibration curve shown in Figure 10. The filled circles represent the data from these fractions for the six different samples. This method was exploited to extend the region spanned by the linear polyester samples to the highest molecular weights possible, since no larger molecular weight linear samples could be made. Even so, these data only extend to molecular weights of about 150 000.

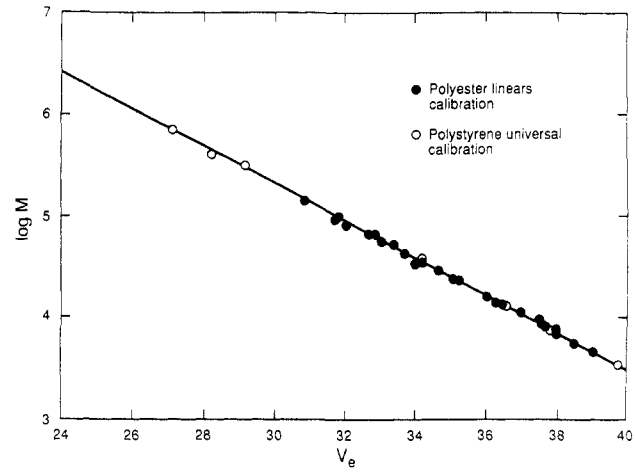

Figure 10. SEC calibration plots of log M versus elution volume V_e in milliliters. Filled circles are from SEC analyses of linear polyester samples, where the molecular weights were calculated for each eluting fraction from the LALLS detector response after band broadening correction. Open circles represent the measurements on narrow distribution polystyrene standards after applying the universal calibration correction (eq 29).

To calibrate the separation of still larger molecular weights, we used several narrow-distribution, linear polystyrene samples (Pressure Chemical Co.) as a second set of standards. Because of their narrow distributions, M_w for a particular standard polystyrene was paired with the elution volume corresponding to the peak maximum of the eluted polymer. The molecular weight of a given polystyrene was rescaled to an equivalent polyester molecular weight using eq 29 and measured Mark–Houwink coefficients of $a = 0.70$ and $K = 1.9 \times 10^{-4}$ dL/g for polystyrene in tetrahydrofuran. These points are indicated in Figure 10 by open circles. The excellent fit of these two curves to each other in the overlapping molecular weight region indicates that this plot correctly represents the calibration curve for polyesters over the entire region. Having established the relationship between hydrodynamic size and elution volume by calibrating with linear polymers, the size–molecular weight relationship can now be determined for the branched polymers.

The log M versus V_e relationship for the fractionated branched materials is illustrated in Figure 11 for three representative high molecular weight samples, along with the calibration curve established for linear polyesters (plotted as a solid line in the figure). The high molecular weight branched polymers demonstrate the expected property of having a larger molecular weight than a linear polymer with the same hydrodynamic volume (same elution volume), and the dependence of log M on V_e is approximately linear over most of the active separation range of the column set for both branched and linear polymers. Although it is not shown in this figure, below a molecular weight of approximately 10 000 the curves for branched

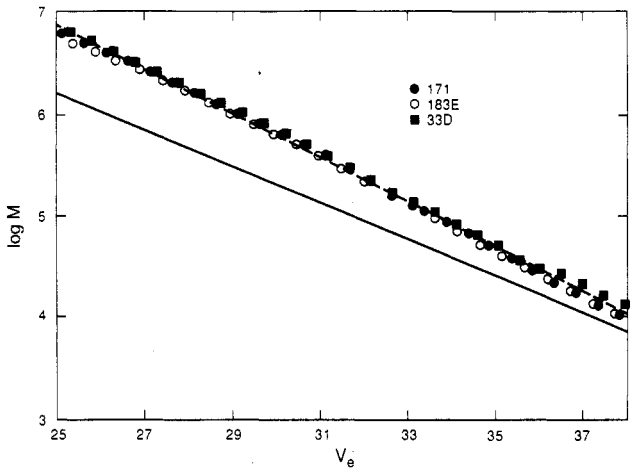

Figure 11. log M versus V_e in milliliters for three branched samples from SEC monitored with LALLS; two samples are from the 0.025 MFBA series and one (33D) from the 0.05 MFBA series. The plots are colinear. The line generated by the linear calibration is included for comparison.

polymers and linear polymers merge. Presumably, this results from the fact that the branch agent is relatively dilute in both series. On average, a 5000 molecular weight chain is expected between each branch site in the 0.025 MFBA polymers (2500 in the 0.05 MFBA samples), so the effects of branching are not expected to be observable in chains with molecular weights less than 5000 in the 0.025 MFBA samples. While we anticipated that the 0.05 MFBA samples would display this behavior at approximately 2500 molecular weight, experimentally no difference is discernible between the two branch agent concentrations; the linear regression lines through the three individual data sets in Figure 11 are statistically identical. Low extent of reaction samples, such as 183B or 183C from the 0.025 MFBA series, gave log M versus V_e curves that were indistinguishable from the linear curves, but of course, these curves did not extend to very high molecular weights. Virtually all other samples were described by the curve defined by the three branched samples in Figure 11, and we only rarely observed a sample with intermediate behavior (183D was one such sample). These results suggest that there is a narrow crossover between linear and branched polymer behavior as observed in this experiment.

The fact that all the higher molecular weight branched samples are described by a single slope in their log M versus V_e behavior suggests that a single unique value of ν^B exists. Again, on the basis of the Daoud and Joanny prediction[26] discussed earlier, we expect that differences between the calibration curves for the two MFBA levels examined will be undetectable. We have evaluated ν^B from the SEC data as follows. Starting with eq 28 and the basic premise of this experiment, namely, that at any given elution volume the hydrodynamic volumes of a branched and a linear polymer must be the same ($R_{L1}^3 = R_{B1}^3$), it is straightforward to show that

$$(M_{L1}/M_{L2})^{\nu^L} = R_{L1}/R_{L2} = R_{B1}/R_{B2} = (M_{B1}/M_{B2})^{\nu^B} \quad (30)$$

where subscripts 1 and 2 designate values at two different elution volumes. With no further assumptions, the ratio ν^L/ν^B can be evaluated from

$$\nu^L/\nu^B = \log (M_{L1}/M_{L2})/\log (M_{B1}/M_{B2}) = \text{slope}_L/\text{slope}_B \quad (31)$$

where slope_L and slope_B are the slopes of the calibration curves for the linear and branched polyester samples, respectively. The linear polymer slope was calculated to be -0.181 ± 0.004. The branched polymer slope was similarly evaluated for the three samples simultaneously and found to be -0.218 ± 0.003. The ratio of ν^B to ν^L is then 0.83 ± 0.03, which agrees perfectly with the predicted ratio from Table I.

The value of ν^B can be found, if ν^L is known. If we assume that the form of the Flory–Fox relation in eq 27 is correct, then the combination of the Mark–Houwink exponent determined for the linear polyesters from Figure 8 with eq 28 yields a value of 0.56 ± 0.01 for ν^L. The value of ν^B is then readily calculated, and we obtain a value of

$$\nu^B = 0.83\nu^L = 0.46 \pm 0.03 \quad (32)$$

This value is in satisfactory agreement with the value of ν^B obtained for unfractionated samples in the Results. The values of ν for both linear and branched polyesters obtained by this method are between the good- and Θ-solvent predictions for these values. The most probable explanation for this result is that tetrahydrofuran is only an intermediate quality solvent for these polyesters. Alternatively, since both ν^B and ν^L are calculated from the Mark–Houwink exponent for polydisperse linear polyesters, we must consider whether the value for this exponent could be anomalously low. If the dispersities of the linear polyesters were identical, then the observed exponent should be the same as the single-chain value. As seen in Table V, the measured dispersities are quite similar, so it is unlikely that they affected the calculations. Another possibility is that we have not reached the high molecular weight limit required by theory, so we are actually observing a crossover value for the exponent, as treated in the framework of the renormalization group theory.[42] The data available are insufficient to resolve these possibilities.

The exponent τ is obtainable from the shape of the distribution function described by eq 7 and from an evaluation of the interdependence of M_w and a molecular weight characterizing the cutoff of that distribution. A dramatic feature near the gel point should be the power law slope, where $P(M,p)$ varies as $M^{-\tau}$, over a large range of molecular weights, as pointed out by Von Schulthess et al.[24] Leibler and Schosseler[18] exploited the characteristic molecular weight method. They approximated the characteristic molecular weight, M_{char}, as the molecular weight corresponding to the peak in the light scattering trace, which they have defined as M_{max}.[18] They were then able to obtain τ from the following scaling relation:

$$M_w \sim M_{char}^{3-\tau} \sim M_{max}^{3-\tau} \quad (33)$$

which results from simple algebra involving eq 4, 6, and 10. We have evaluated τ by both methods for our branched polyester system.

The starting point for this analysis is the combination of concentration and light scattering detector outputs, illustrated for three samples from the 0.025 MFBA series in Figure 12, where both detector signals are plotted versus elution volume. The characteristic features reported previously for the cross-linked polystyrene solutions[18] are also demonstrated by these polyesters. Specifically, the peak molecular weight in the concentration detector traces remains relatively constant, but there are progressively larger amounts of material extending to higher molecular weights as p_c is approached; the distributions become increasingly broad. However, the peak in the LALLS output increases in both molecular weight and size as the gel point is approached. The peak in the LALLS trace is close to the extreme high molecular weight end of the distribution. M_{max} is obtained directly from this peak position after converting elution volume to molecular weight.

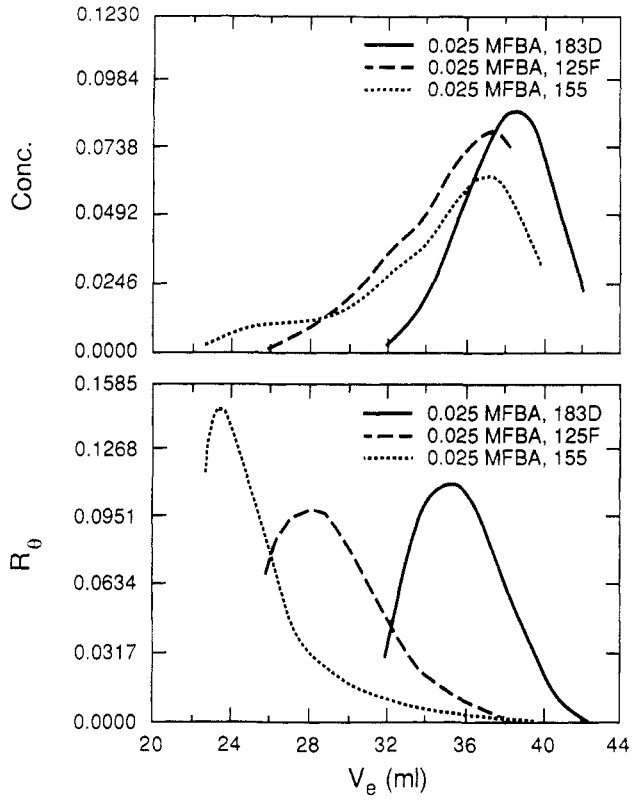

Figure 12. Concentration curves monitored with a refractive index detector and R_θ, scattering intensity, curves monitored with LALLS for three samples containing 0.025 MFBA, plotted versus elution volume. As the polymer grows toward gelation, the molecular weight distribution broadens, with the amount of material eluting at the low elution volume (high molecular weight) end of the chromatogram increasing. The traces from the LALLS detector indicate dramatically the shift of the highly scattering component of the total polymer distribution to higher molecular weights. The curves in each figure were nomalized to a constant area, so that the relative shapes can be more easily compared. The scattering signal from samples close to the gel point is much larger than that from a sample early in the reaction.

The chromatographic data are essentially equally spaced on a logarithmic molecular weight scale. Therefore, we must convert the chromatographic information in the function $C(V_e)$ to an equivalent function based on a linear molecular weight scale to correspond to the scaling function $\phi(M,p)$, which Leibler and Schosseler[18] have defined as

$$\phi(M,p) \sim MP(M,p) \tag{34}$$

A proportionality has been indicated to avoid dealing with the normalization prefactors for the functions $\phi(M,p)$ and $P(M,p)$. Leibler and Schosseler[18] defined $\phi(M,p)$ in terms of $C(V_e)$ according to

$$\sum_{i=1}^{j} C_i = \int_0^{M_j} \phi(M,p)\, dM \tag{35}$$

where i is the index for stepping through the experimental profile of $C(V_e)$. We have evaluated the function $\phi(M,p)$ at each volume increment by dividing C_i by the quantity $M_i - M_{i-1}$, starting from the low molecular weight end of the distribution. For $i = 1$, we have taken M_{i-1} to be 0. While evaluating $\phi(M,p)$ in this manner imposes a systematic shift of the distribution to lower molecular weights, the effect is small compared to the error estimates on M_{char} values, and the exponent τ is unaffected by the shift.

Examples of the resulting $\phi(M,p)$ functions are shown in Figure 13 for the same three data sets as used in Figure 12. The power law region of the data is clearly evident in

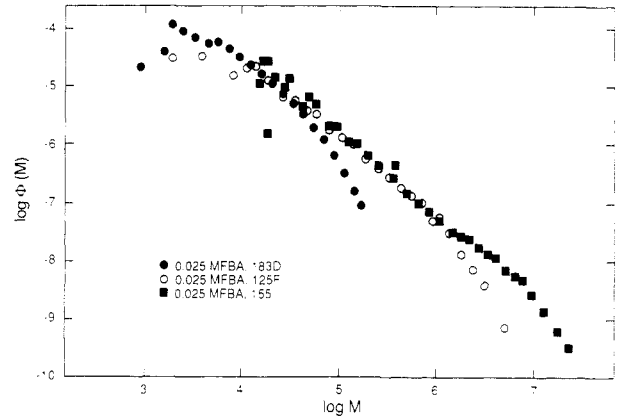

Figure 13. log $\phi(M,p)$ versus log M for the three data sets shown in Figure 12, illustrating the power law behavior of the high molecular weight portions of these samples. Data at the low molecular weight end of the plots is scattered because of the weakness of the light scattering intensity at this end of the distribution. At the high molecular weight end, the LALLS signal is strong, but the concentration signal falls to baseline, making it difficult to describe accurately the shape of the molecular weight cutoff function (eq 7).

the higher extent of reaction samples (183E and 155), and the effects of the molecular weight cutoff function are evident at the high molecular weight end of each distribution. There is also evidence of the expected fall off in the low molecular end of each distribution. Unfortunately, this effect is convoluted with an experimental problem, namely, that the light scattering signal falls below the noise level well before the concentration goes to zero at the low molecular weight end. The net result is that the molecular weights are imprecisely determined for the first few data points. Since our interest is in the scaling behavior of the distribution at high molecular weights anyway, we have chosen to ignore the first few data points in subsequent analyses. In terms of the concentration detector output in Figure 12, the discarded data correspond roughly to the portion of the distribution to the low molecular weight side of the peak. The data at the high molecular weight end of the distribution suffer the reverse situation, i.e., the concentration detector output falls to the baseline, although the scattering detector still has significant signal. While the higher signal-to-noise ratio for the concentration detector prevents the difficulties in molecular weight determinations, the low concentration signal limits our ability to describe accurately the shape of the cutoff function.

Because of the limitations cited above at both extremes of the observed distributions, the various data sets have been simultaneously fit to a function of the form

$$\ln \phi\ (M,p) = \ln A - (\tau - 1) \ln M - \frac{M}{M_{char}(p)} \tag{36}$$

where ln A and τ then are averaged over all of the data sets listed in Table VI, but each data set has a unique value of $M_{char}(p)$. We do not mean to imply here that we expect a constant prefactor A at different extents of reaction. In fact, we expect that the function $\phi(M,p)$ must go through a maximum and begin decreasing again as the molecular weight decreases. However, for the portion of the distributions we have included in this analysis, fits to individual data sets yielded a single value of A within the uncertainties on that parameter, so we treated it as a constant to minimize the number of fitting parameters. At the high molecular weight end of the distribution, a simple exponential cutoff function was used for this analysis, because the limited data available in the cutoff region makes interpretation of a more complicated function questionable.[43]

Table VI
Summary of Distribution Function Fit Results

$\ln A = 1.7 \pm 0.2$; $\tau = 2.30 \pm 0.02$

sample	M_{char}[a]	M_w[b]	M_{max}[c]
	0.025 MFBA Samples		
155	$(2.0 \pm 1.0) \times 10^7$	7.8×10^5	$(1.4 \pm 0.3) \times 10^7$
171	$(5.4 \pm 1.2) \times 10^6$	3.7×10^5	$(4.9 \pm 1.2) \times 10^6$
183E	$(5.0 \pm 1.0) \times 10^6$	2.8×10^5	$(3.7 \pm 0.4) \times 10^6$
183D	$(8.7 \pm 1.8) \times 10^4$	1.6×10^4	$(3.8 \pm 0.5) \times 10^4$
125F	$(2.6 \pm 0.4) \times 10^6$	1.1×10^5	$(1.1 \pm 0.2) \times 10^6$
125E1	$(1.4 \pm 0.1) \times 10^5$	2.0×10^4	$(8.8 \pm 1.9) \times 10^4$
125D	$(5.1 \pm 1.7) \times 10^4$	9.5×10^3	$(2.0 \pm 0.2) \times 10^4$
173	$(2.8 \pm 0.4) \times 10^5$	3.4×10^4	$(1.4 \pm 0.2) \times 10^5$
	0.05 MFBA Samples		
191D	$(5.4 \pm 0.6) \times 10^4$	9.9×10^3	$(2.7 \pm 0.6) \times 10^4$
191E	$(9.0 \pm 1.8) \times 10^4$	1.2×10^4	$(3.6 \pm 0.8) \times 10^4$
191F	$(2.9 \pm 0.3) \times 10^5$	3.2×10^4	$(1.3 \pm 0.4) \times 10^5$
91C	$(6.6 \pm 1.0) \times 10^4$	1.2×10^4	$(3.8 \pm 1.0) \times 10^4$
91D	$(1.7 \pm 0.2) \times 10^5$	2.2×10^4	$(1.0 \pm 0.3) \times 10^5$
91E	$(5.9 \pm 1.1) \times 10^5$	5.7×10^4	$(4.0 \pm 1.1) \times 10^5$
33D	$(1.7 \pm 0.7) \times 10^7$	6.6×10^5	$(7.0 \pm 0.8) \times 10^6$

[a] Uncertainies represent standard estimates of 95% confidence intervals with Student's t distribution. [b] Since M_w values are derived from standard light scattering measurements, uncertainties of ±10% have been assumed for these values, typical values for this technique. [c] Uncertainties are based on the spacings between adjacent points in the digitized chromatograms and, therefore, overestimate the uncertainty in the peak position.

The fit results reported below were obtained with both 0.025 and 0.05 MFBA series samples included, but to guarantee that the fit parameters actually describe both sets, the two MFBA series, as well as other subsets of these series, were fit separately to the same model function.

All of the various combinations of data sets gave essentially identical results for ln A, τ, and $M_{char}(p)$ except for the M_{char} value for sample 155 in the 0.025 MFBA series. Evidently, the cutoff function f' was less well defined in the high molecular weight end of this data set, leaving some ambiguity as to the best value for M_{char}. We settled on a value of $(2 \pm 1) \times 10^7$ for M_{char} in this sample. Fits of eq 36 to individual data sets gave equivalent results for high extent of reaction samples for all parameters, but τ and ln A values from individual fits showed some systematic deviations in low-p samples. We attributed this problem to the absence of a well-developed power law region for intermediate molecular weights in these samples, as illustrated for the 183D sample in Figure 13; these apparent deviations in τ and ln A were discounted for that reason. The values of ln A and τ were found to be 1.7 ± 0.2 and 2.30 ± 0.02, respectively. The value of τ obtained here is in good agreement with that determined above through the scaling relations involving unfractionated samples. The values of M_{char} for each individual data set are shown in Table VI, along with the M_{max} and M_w values for each set. Estimates of the uncertainties for each of these parameters are also listed in Table VI.

With the fit results for M_{char}, we are able to test the assumption of M_{max} scaling directly as M_{char}, as described by Leibler and Schosseler,[18] and evaluate τ by their method. The comparison of M_{max} to M_{char} is illustrated in a log–log plot of the former versus the latter in Figure 14. As expected based on earlier observations, there is no distinction between the different MFBA levels. Linear regression analysis of these data indicates that the scaling exponent relating these two molecular weights is indistinguishable from unity within 95% confidence statistical limits, where M_{max} was found to vary as $M_{char}^{1.05\pm0.07}$. Figure 15 shows the comparison of M_{max} to M_w in a log–log format. This line has a slope defined as $1/(3 - \tau)$, and

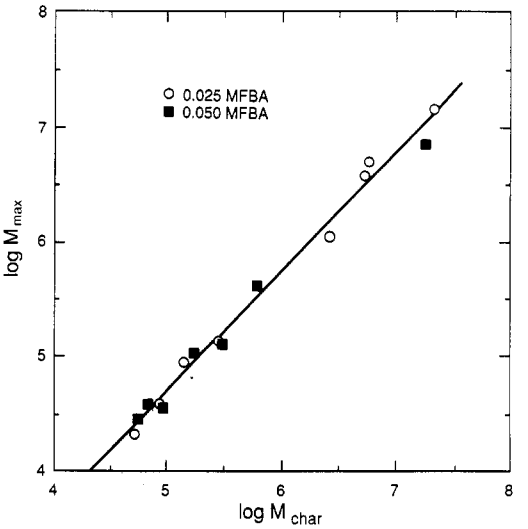

Figure 14. Plot of log M_{max} versus log M_{char}. The slope of this plot is 1.05 ± 0.07 at 95% confidence, indicating that these two parameters are directly proportional to one another.

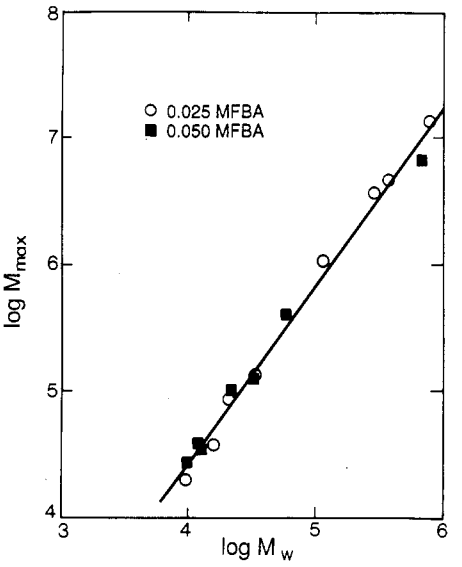

Figure 15. log M_{max} is plotted against log M_w in this figure, and the fit line has a slope of 1.43 ± 0.08. According to theory, this slope should be equal to $1/(3 - \tau)$, which leads to a value of τ of 2.30 ± 0.04.

regression analysis yields a slope of 1.43 ± 0.08, and hence $\tau = 2.30 \pm 0.04$ at 95% confidence, which agrees perfectly with the τ values obtained from other experimental measures of this system.

It has been pointed out that if the scaling law holds (eq 7), then the funtion $G(M/M_{char})$, defined as

$$G\left(\frac{M}{M_{char}}\right) = M_{char}^{(\tau-1)}\phi(M,p) \qquad (37)$$

must be a universal function of M/M_{char}, independent of the extent of reaction.[18] We have tested this concept with this system, as shown in Figure 16 in a plot of log $G(M/M_{char})$ versus log M/M_{char}. This format was chosen over the one used by Leibler and Schosseler[18] to emphasize the intermediate molecular weight ranges, or power law region, where the precision of the data is the best (since both the LALLS and concentration detector signals are large throughout this region). All 15 distribution functions are shown in this figure, as well as the normalized fit line from eq 36. The universal nature of the scaling function is dramatically demonstrated here for the high molecular

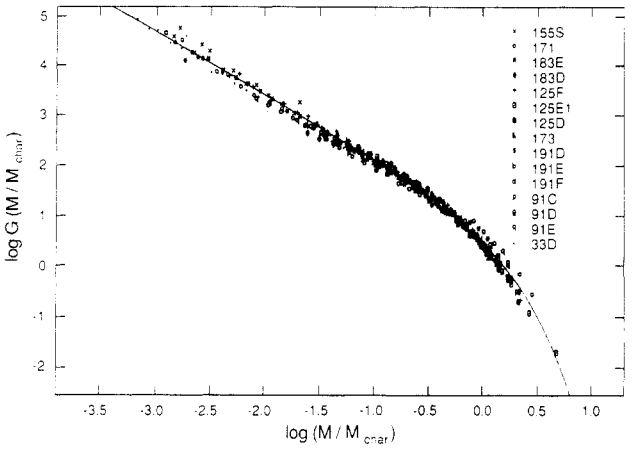

Figure 16. log $G(M/M_{char})$ versus log (M/M_{char}) for all 15 distribution functions. This plot demonstrates the universality of the scaling function (eq 37) for the high molecular weight portions of the distributions.

weight portion of the distributions from both MFBA levels. Independent of any discussions of the relative merits of critical exponents analyses,[44] the demonstration of such a universal function provides a powerful characterization tool for describing gelling polymer systems.

Discussion

The most significant experimental result in this gelation study is the demonstration that scaling relationships are obeyed by these polyesters. In fact, the scaling relationships apply over broader ranges of molecular weights or extents of reaction than was expected in experiments on either fractionated or unfractionated samples. No significant deviations from scaling behavior were observed for even very low extent of reaction samples. Through examinations of these scaling behaviors, we were able to obtain estimates of the scaling exponent ν^B by two independent methods, of the critical exponent τ by three independent methods, and of the critical exponent γ by one method. We found good agreement between the independent measures of ν^B and τ, indicating that this analysis scheme is internally consistent.

If we take the average of the two results as the best value, we find ν^B to be 0.48 ± 0.02 for this system. In addition, we were able to show that the ratio of ν^B to ν^L agreed with the theoretically predicted ratio. The theoretical prediction of 0.5 is at the upper bound of the 95% confidence interval on this value, so it seems likely that our value is slightly less than the theoretical prediction. Our result bears the same relationship to the measurements of Bouchaud et al.[19] and Adam et al.,[20] where they found $\nu^B = 0.505 \pm 0.005$ for a polyurethane system, in exact agreement with theory. As pointed out earlier, we think our result implies that tetrahydrofuran is only an intermediate quality solvent for our polyester system. The measurement of Leibler and Schosseler,[39] $\nu^B = 0.41 \pm 0.05$, does not agree with our work or that of the other workers.[19,20] On the other hand, the results of Kajiwara et al.[33] and Burchard et al.[36] would lead to a wide range of values for ν^B, using eq 14 and assuming a reasonable value for τ, for a single polymer–solvent combination. While this behavior would also seem unlikely, it is apparent that more experiments will be needed to test the theoretical predictions for ν^B.

The simple average of the three τ observations yields a value of 2.29 ± 0.03, which is much closer to the percolation prediction than to the classical result. Our result clearly disagrees with the Flory–Stockmayer prediction, but whether it is distinguishable from the percolation result depends on the precise definition of the uncertainty in the statistical evaluation of this theoretical value.[45] Our result agrees well with the value observed for cross-linked polystyrenes by Leibler and Schosseler,[18] but it is marginally different than the value observed in polyurethanes,[19,20] where the percolation result was obtained exactly. The value of τ obtained by von Schulthess et al.[24] of 1.4 is clearly different, but they have argued that this is the expected value for their system.

Table VII
Summary of Scaling and Critical Exponents

Critical Exponents of Gelation Transition

exponent	percolation	Flory–Stockmayer	exptl
τ	2.20	2.5	2.29 ± 0.03
γ	1.74	1	1.8 ± 0.3
β	0.45	1	0.7 ± 0.2
σ	0.46	0.5	0.40 ± 0.08
ν_p	0.88	0.5	1.1 ± 0.2

Scaling Exponents in Good Solvents

exponent	prediction	exptl
ν^B	0.5	0.48 ± 0.02
ν^L	0.6	0.56 ± 0.01

The value of γ was found to be 1.8 ± 0.3, which agrees perfectly with the percolation result, as well as three previous experimental results.[20,24,33] The Kajiwara et al.[33] result of 1.0 for a bulk-polymerized polyurethane is hard to rationalize with our result, since these two systems differ mainly through the existence of the reequilibration process in our system. Flory[16] has argued that this feature should not matter in a step-growth-type polymerization, but we can see no other significant system property to account for the different γ observations.

While the percolation predictions are clearly favored by our observations of these critical exponents, the evidence is not definitive. Some aspects, such as the applicability of the distribution function to such a wide variation in the extent of reaction, indicate classical behavior. Because the wide spacing between cross-links relieves the packing constraints in three dimensions that are normally expected to lead to percolation-type behavior, this system may exhibit some crossover behavior[46] between percolation, which is observed in densely cross-linked systems, and Flory–Stockmayer predictions, which are expected in vulcanization reactions.[47,48] The widely separated cross-links may account for the better agreement of this work with that of Leibler and Schosseler[18] than with that of the other workers.[19,20]

From the two measured exponents and eq 9 and 10, values for σ and β are calculated and reported in Table VII. To obtain the third exponent, ν_p, necessary to complete the set of three static exponents of this universality class, we must assume hyperscaling. (Again, we remind the reader that ν_p is not related to the exponent ν, defined by $R \sim M^{\nu}$.) The third exponent ν_p is defined in the relationship between the characteristic length in the system, ξ, and the distance from the gel point by

$$\xi \sim |p - p_c|^{-\nu_p} \tag{38}$$

Hyperscaling can be expressed as[14]

$$d\nu_p = \gamma + 2\beta = \frac{\tau - 1}{\sigma} \tag{39}$$

which relates ν_p and dimensionality of space, d, to the two measured exponents. We find the value of ν_p to be 1.1 ± 0.2, which again is more consistent with percolation than Flory–Stockmayer predictions. But it is important to remember that the hyperscaling assumption is not valid for

the Flory–Stockmayer theory. The various exponents are summarized in Table VII.

Independent of the discussion of theoretical predictions, there are several interesting experimental features highlighted by this analysis. Probably the most significant of these is the demonstration of the universal distribution function $G(M/M_{char})$ in Figure 16. Since this function describes the data at all reasonable extents of reaction in this system, any new sample could be completely characterized by determining any one fixed parameter, such as p or M_w, and calculating the rest from $G(M/M_{char})$ and known relationships between the variables.

Acknowledgment. We gratefully acknowledge the experimental support of James Whitefield, Lan Thai, and Frank Pettrone and helpful discussions with Drs. Ludwig Leibler, Mireille Adam, and Walther Burchard. We also appreciate the thoughtful comments from the reviewers.

Registry No. (Dimethyl glutarate)(dimethyl terephthalate)(neopentyl glycol)(pentaerythritol) (copolymer), 117942-61-7.

References and Notes

(1) Flory, P. J. *J. Am. Chem. Soc.* **1941**, *63*, 3083, 3091, 3096.
(2) Stockmayer, W. H. *J. Chem. Phys.* **1943**, *11*, 45; **1944**, *12*, 125.
(3) de Gennes, P.-G. *J. Phys. Lett.* **1976**, *37*, L1.
(4) Stauffer, D. *J. Chem. Soc., Faraday Trans. 2* **1976**, *72*, 1354.
(5) Broadbent, S. R.; Hammersley, J. M. *Proc. Camb. Philos. Soc.* **1957**, *53*, 629.
(6) Manneville, P.; de Seze, L. In *Numerical Methods in the Study of Critical Phenomena*; Della Dora, I., Lacolle, B., Eds.; Springer: Berlin, 1981.
(7) Herrmann, H. J.; Landau, D. P.; Stauffer, D. *Phys. Rev. Lett.* **1982**, *49*, 412.
(8) Basin, R.; Hermann, H. J.; Stauffer, D. *J. Polym. Sci., Polym. Symp.* **1985**, *73*, 175.
(9) Nossal, R. *Macromolecules* **1985**, *18*, 49.
(10) Meakin, P. *Phys. Rev. Lett.* **1983**, *51*, 1119.
(11) Kolb, M.; Jullien, R.; Botet, R. *Phys. Rev. Lett.* **1983**, *51*, 1123.
(12) Essam, J. W. *Rep. Prog. Phys.* **1980**, *43*, 833.
(13) Stauffer, D. *Introduction to Percolation Theory*; Taylor & Francis: Philadelphia, 1985.
(14) Stauffer, D.; Coniglio, A.; Adam, M. *Adv. Polym. Sci.* **1982**, *44*, 103.
(15) Herrmann, H. *Phys. Rep.* **1986**, *136*, 157.
(16) Flory, P. J. *Principles of Polymer Chemistry*; Cornell University Press: Ithaca, NY, 1953.
(17) Brauner, U. *Makromol. Chem.* **1979**, *180*, 251.
(18) Leibler, L.; Schosseler, F. *Phys. Rev. Lett.* **1985**, *55*, 1110. (See also: Schosseler, F.; Benoit, H.; Gallot, Z.; Strazielle, Cl.; Leibler, L. Submitted for publication in *Macromolecules*.)
(19) Bouchaud, E.; Delsanti, M.; Adam, M.; Daoud, M.; Durand, D. *J. Phys. (Les Ulis, Fr.)* **1986**, *47*, 1273.
(20) Adam, M.; Delsanti, M.; Munch, J. P.; Durand, D. *J. Phys. (Les Ulis, Fr.)* **1987**, *48*, 1809.
(21) Stanley, H. E. *Introduction to Phase Transition and Critical Phenomena*; Clarendon Press: Oxford, 1971.
(22) Patton, E. V.; Wesson, J. A.; Hewitt, P. M.; Wilson, J. C.; Whitefield, J. submitted for publication in *Macromolecules*.
(23) Essam, J. W.; Gwilym, K. M. *J. Phys.* **1971**, *C4*, L228.
(24) von Schulthess, G. K.; Benedek, G. B.; De Blois, R. W. *Macromolecules* **1980**, *13*, 939.
(25) Isaacson, J.; Lubensky, T. C. *J. Phys. Lett.* **1980**, *41*, L469.
(26) Daoud, M.; Joanny, J. F. *J. Phys. (Les Ulis, Fr.)* **1981**, *42*, 1359.
(27) Daoud, M.; Family, F.; Jannink, J. *J. Phys. Lett.* **1984**, *45*, L199.
(28) de Gennes, P.-G. *Scaling Concepts in Polymer Physics*; Cornell University Press: Ithaca, NY, 1979.
(29) Burchard, W.; Kajiwara, K.; Gordon, M.; Kalal, J.; Kennedy, J. W. *Macromolecules* **1973**, *6*, 642.
(30) Kim, C. J.; Hamielec, A. E.; Benedek, A. *J. Liq. Chromatogr.* **1982**, *5*, 425.
(31) Mori, S. *J. Appl. Polym. Sci.* **1977**, *21*, 1921.
(32) Burchard, W. Private communication.
(33) Kajiwara, K.; Burchard, W.; Kowalski, M.; Nerger, D.; Dusek, K.; Matejka, L.; Tuzar, Z. *Makromol. Chem.* **1984**, *185*, 2543.
(34) We have estimated the ratio of R_h to Rg to be 0.51 ± 0.17 based on the distance between the two fit lines in the middle of the data range, with the error bar corresponding to the widest excursions of the data from these lines. Theoretically, this value is not very precisely defined[35] because of ambiguity associated with the nature of segment density at the edges of a branched polymer structure. Expectations are that for randomly branched structures such as these the ratio of R_h to R_g should approach or even exceed unity[36] due to the relatively larger segment density in the center of the branched structure and its effect on hydrodynamic properties. There are several relevant experimental measures available that provide useful comparisons. Schmidt and Burchard[37] found this ratio to be 0.79 ± 0.04 for linear polystyrenes in Θ solvents, which have the same theoretical fractal dimensionality as a branched polymer in a good solvent (the fractal dimensionality is given by ν^{-1}; see Table I). Wiltzius[38] reported a value of 0.72 ± 0.02 for colloidal silica aggregates in an aqueous salt solution, which should have a random branching architecture. Burchard et al.[36] reported a value in the range of 0.77 ± 0.06 for branched epoxy polymers, and Kajiwara et al.[33] found the ratio to be approximately 0.5 for solution polymerized branched polyurethanes and 1.25 for bulk polymerized samples, in what should be the best comparisons to our system. We are unable to reconcile our result with these other measurements at this time, although there is clearly no unanimity in these data about the variation of this ratio with branching.
(35) Van Saarloos, W. *Physica* **1987**, *147A*, 280.
(36) Burchard, W.; Bantle, S.; Wachenfeld-Eisele, E. *Makromol. Chem., Makromol. Symp.* **1987**, *7*, 55.
(37) Schmidt, M.; Burchard, W. *Macromolecules* **1981**, *14*, 210.
(38) Wiltzius, P. *Phys. Rev. Lett.* **1987**, *58*, 710.
(39) Leibler, L.; Schosseler, F. In *Physics of Finely Divided Matter*; Boccara, N., Daoud, M., Eds.; Springer-Verlag: Berlin, 1985; p 135.
(40) Fox, T. J., Jr.; Flory, P. J. *J. Phys. Colloid Chem.* **1949**, *53*, 197.
(41) Grubisic, Z.; Rempp, P.; Benoit, H. *J. Polym. Sci., Part B* **1967**, *5*, 753.
(42) Oono, Y. *Adv. Chem. Phys.* **1985**, *61*, 301.
(43) A stretched exponential functional form was also used for the simultaneous fitting procedure defined as $\ln\{\phi(M,p)\} = \ln A' + (1-\tau)\ln M - cM^{\zeta}$, where A' is the constant prefactor, c is related to $M_{char}^{-\zeta}$, and ζ is the stretch exponent. The best fit to the data was obtained with $\zeta = 1.0 \pm 0.5$, and there was no reduction in the sum of squared residuals values. The quality of the fit was not very sensitive to the value of ζ, and we found $c = M_{char}^{-\zeta}$ within the typical bounds for these values. On this basis, we concluded that a simple exponential cutoff function was most appropriate for fitting the observed distribution functions, especially given the fewer unconstrained parameters.
(44) Gordon, M.; Torkington, J. A. *Pure Appl. Chem.* **1981**, *53*, 1461.
(45) Stanley, H., private communication.
(46) Alexander, S. In *Physics of Finely Divided Matter*; Boccara, N., Daoud, M., Eds.; Springer-Verlag: Berlin, 1985; p 185.
(47) de Gennes, P.-G. *J. Phys. Lett.* **1977**, *38*, L355.
(48) Daoud, M. J. *J. Phys. Lett.* **1979**, *40*, L201.